PCCP

Accepted Manuscript

This is an *Accepted Manuscript*, which has been through the Royal Society of Chemistry peer review process and has been accepted for publication.

Accepted Manuscripts are published online shortly after acceptance, before technical editing, formatting and proof reading. Using this free service, authors can make their results available to the community, in citable form, before we publish the edited article. We will replace this *Accepted Manuscript* with the edited and formatted *Advance Article* as soon as it is available.

You can find more information about *Accepted Manuscripts* in the Information for Authors.

Please note that technical editing may introduce minor changes to the text and/or graphics, which may alter content. The journal's standard Terms & Conditions and the Ethical guidelines still apply. In no event shall the Royal Society of Chemistry be held responsible for any errors or omissions in this *Accepted Manuscript* or any consequences arising from the use of any information it contains.

ROYAL SOCIETY OF CHEMISTRY

www.rsc.org/pccp

Please do not adjust margins

Journal Name

ARTICLE

Received 00th January 20xx,
Accepted 00th January 20xx

DOI: 10.1039/x0xx00000x

www.rsc.org/

Role of ambient ice-like water adlayers formed at the interfaces of graphene on hydrophobic and hydrophilic substrates probed using scanning probe microscopy

Thavasiappan Gowthami, Gopal Tamilselvi, George Jacob and Gargi Raina*

In this work, we report the role of ice-like water adlayers (IWL) formed under ambient in between mechanically exfoliated as-prepared and patterned few layer graphene (FLG) and multi-layer graphene (MLG) on hydrophobic Si and hydrophilic SiO_2/Si substrates. The growth of the IWL is probed by measuring the height changes in graphene using intermittent contact atomic force microscopy (IC-AFM) and their electrostatic effect is studied using electrostatic force microscopy (EFM) over time. It is found that more IWLs are formed within shorter period of time, when both as-prepared graphene and underlying substrates are either hydrophobic or hydrophilic in nature. In contrast, AFM voltage nanolithographically patterned trenches on FLG and MLG on Si substrate, show quick formation of IWL. The effect of IWL formed, on the dimensions of trenches, is correlated with the variation of the measured EFM phase shift over time. This study demonstrates the dependence of the formation of IWLs under ambient on the affinity towards water, at the interface of graphene on hydrophobic and hydrophilic substrates, which has important implications for the performance of graphene-based nanoelectronics devices.

1. Introduction

Graphene, as a novel 2D-nanomaterial since its isolation by a simple method,[1] has become one of the most researched material with wide and far reaching applications in various fields of nanoelectronics devices,[2-6] photovoltaics,[7] sensors,[8,9] and plasmonics.[10] Most graphene-based devices will require operation under ambient, however the presence of ambient adsorbate layers will significantly affect the performance of the device by altering the doping[11-14] and the mobility profiles due to changes in charge carrier density.[14,15]

The presence of ambient water adlayers between graphene (different layer thickness) on different insulating substrates such as mica,[11, 14, 16-20] SiO_2,[21-25] BaF_2,[26] CaF_2,[26, 27] SiC[12] and Sapphire[13] as well as metal substrates viz. Ni[28], Ru and Cu[29] and semiconducting Si substrate[30] have been reported. Xu *et al.*[16] were the first to visualize water adlayers at room temperature using atomic force microscopy (AFM) by graphene templating on mica and reported the formation of faceted domains with height corresponding to a monolayer of ice-like water (0.37 ± 0.02 nm). It was reported by Shim *et al.*[14] that the interfacial monolayer of ice-like water between single layer graphene on mica is stable upto a year, causing a permanent p-type doping of graphene. Using scanning tunneling microscopy (STM) study of few layered water trapped between monolayer of graphene and mica at room temperature, it was found that while the first water-adlayer is crystalline, subsequent second and third layers are amorphous.[17] The role of different types of adhesive tapes in the formation of molecular water adlayers between graphene and mica was also investigated by Rezania *et al.*[18] and was found that there is slight difference in the growth from tape to tape. Kim *et al.*[19] studied wetting and diffusion phenomenon of water adlayer between single layer graphene (SLG), bi-layer graphene (BLG) and few layer graphene (FLG) and hydrophilic mica under ambient relative humidity (RH) of ~50% and reported that the first monolayer of IWL strongly adheres beneath the graphene surface and additional intercalated water adlayer gets aligned along the zig-zag directions of graphene. Ochedowski *et al.*[11] studied doping characteristics of graphene on mica with intercalated water adlayers, by performing a thermal treatment in UHV. They showed that the intercalated water adlayers are partially removed under mild heating (200°C) and the defect density increases leading to 'nanoblisters' formation at temperatures of 600°C causing a transition from p-type to n-type for graphene layer.[11] Nanomanipulation of liquid-like water droplets trapped

Center for Nanotechnology Research, VIT University, Vellore 632014, India.
*E mail: gargiraina@vit.ac.in
† Electronic Supplementary Information (ESI) available: Plots of EFM phase shift values for un-patterned regions of FLG, MLG and FLG trench 1, MLG trench 2 patterns with time. See DOI: 10.1039/x0xx00000x

Please do not adjust margins

Physical Chemistry Chemical Physics Accepted Manuscript

between graphene and mica is possible only in the regions where the ice-like water adlayer is present.[20]

Many studies have been performed for graphene on hydrophilic SiO_2 substrate. In 2008, Moser *et al.*[21] demonstrated that the water molecules form strong dipole layer on graphene and characterized the electrostatic environment using electrostatic force microscopy. It has been reported that the surface potential of graphene in ambient, is suppressed due to ambient adsorbates in comparison to graphene on SiO_2 under vacuum.[23] In addition, the surface potential of graphene flakes increases with increasing number of graphene layers.[12,23] Lee *et al.*[24] report that under ambient conditions, first a stable bi-layer of ice-like structure is formed in between graphene and SiO_2 substrate over a week's exposure, followed by liquid phase water formation upon one additional week's exposure, thereby introducing wrinkles and folds in the graphene. The formation of nanopores by thermal oxidation of SLG helps in the quick diffusion of water adlayers.[25] Raman studies of interfacial water between graphene and sapphire substrate point to increasing hole doping in graphene with increasing amount of interfacial water.[13] Verdaguer *et al.*[26] studied the formation of interfacial water adlayers between FLG and insulating BaF_2 and CaF_2 substrates and found that the IWL are formed only in the case of BaF_2 substrate due to less lattice mismatch with hexagonal (I_h) ice. Recently, the formation of stable nanoblisters between graphene and CaF_2 dielectric substrate upon long exposure to ambient humidity, due to pockets of liquid-filled structures, has been reported.[27] Temperature dependence of water adsorption and desorption studies of epitaxially grown graphene on SiC was reported by Kazakova *et al.*[12] and they showed that the surface potential increases with increasing temperature. The hydrophobicity of graphene increases with increasing number of graphene layers.[12]

Wettability transition from hydrophobic to hydrophilic in graphene on Ni substrate was studied using contact angle measurements upon UV irradiation under ambient conditions.[28] Low temperature UHV STM studies of water exposure samples of graphene on Ru and Cu metal substrates, showed discontinuity in Moiré patterns along the line defects in graphene.[29]

There are very few reports of water adlayers sandwiched between graphene and Si substrate. The shift in G and 2D Raman bands and contact potential difference for increasing number of graphene layers was reported for mechanically exfoliated single layer graphene on atomically flat Si (111) under UHV by Ochedowski *et al.*[30].

Recently, we reported the impact of the interaction and dynamics of ambient water adlayers on etch patterns created by AFM voltage nanolithography on hydrophobic highly oriented pyrolytic graphite (HOPG) surfaces.[31] This study demonstrated that the stored electrostatic energy of polarized ice-like water adlayer causes slow etching reaction long after lithography, whereas surrounding liquid-like water droplets do not contribute towards changing dimensions of the etched patterns.[31]

In the present work, we investigate the growth and the effect of the dynamics of ice-like water adlayers under ambient, between mechanically exfoliated few layer graphene (FLG); multilayer graphene (MLG) on hydrophilic (SiO_2/Si) and hydrophobic (Si) substrates and patterned FLG and MLG on Si substrate probed using IC-AFM. It is known that the FLG is hydrophilic in nature while as MLG is hydrophobic.[12] The number of ice-like water adlayers present are more and form over a shorter interval of time when both graphene layers and substrates are of the same nature viz., either both hydrophilic or both hydrophobic. Further, the role of the ice-like water adlayer present between AFM voltage lithographically-modified FLG and MLG on Si substrate is also investigated. The introduction of defects in graphene enhances the quick formation of ice-like water adlayers for both FLG/Si and MLG/Si systems despite the dissimilar nature of FLG and MLG. The modification in the morphology of the lithographic patterns on FLG and MLG on Si with time is correlated with the charge dissipation using EFM, and is attributed to the varying ice-like water adlayers present between graphene and Si substrate. This is the first report bringing out the dependence of growth of ice-adlayers on the relative affinity towards water for as-prepared graphene layers and patterned graphene on technologically important SiO_2/Si and Si substrates. This information is very important towards functionality of graphene-based nanoelectronic devices.

2. Experimental

2.1. Graphene synthesis

Graphene flakes were synthesized using mechanical exfoliation technique,[1] in which a 3M scotch tape was pressed on ZYB grade HOPG, with a mosaic spread of ~0.8°. Thin regions of graphene flakes present in the scotch tape were transferred to a cleaned p-doped Si (100) and n-doped SiO_2/Si (100) substrates with 300 nm thick oxide. The cleaning of the Si and SiO_2/Si substrates was done by sonicating in acetone and iso-propyl alcohol (IPA) to remove the organic contaminants and loose particles on the surface. The number of cleaving and pressing time duration is optimized to transfer minimal number of graphene layers on the above substrates. Tape residues were removed by dipping the samples into acetone and IPA. Mild sonication of samples with IPA results in FLG and MLG flakes with clean surfaces. The dipping and sonication time were optimized to obtain optically clean graphene and substrate surfaces at 1000X magnification. FLG and MLG regions on Si and SiO_2/Si substrates were identified and analyzed with the help of optical microscope (Olympus BX61, Japan) and CP-II AFM (Veeco, USA).

Physical Chemistry Chemical Physics Accepted Manuscript

 This journal is © The Royal Society of Chemistry 20xx

2.2. Graphene patterning using AFM voltage nanolithography

For the lithography process, contact mode AFM was used and conducting tip (SCM-PIT with Pt/Ir coating, resonance frequency 60 kHz, spring constant 1-5 N/m, from Bruker, USA) kept at ground potential and the sample was kept at positive bias. Lithography patterns were created with sample bias of 10V, set-point force of 5nN, tip speed of 0.01µm/s under ambient humidity of 50% RH on graphene on Si substrate by AFM voltage nanolithography using CP-II AFM enclosed in an environmental chamber inside a clean room (Class 1000) atmosphere. A small set-point force of 5 nN was optimized on the mechanically exfoliated FLG samples transferred on Si substrates such that no folding and cutting of edges of FLG takes place while the lithography trench patterns are created.

2.3. Study of ambient water adlayers of graphene using IC-AFM and EFM

IC-AFM imaging was performed using SCM-PIT tip in ambient humidity (RH 50-52%) with free amplitude of cantilever of 70 nm, set-point amplitude of 50-55 nm and drive percentage of 7-8%, so as to avoid unstable operation due to random tip 'snap-ins' caused by ambient water adlayers as well as minimal perturbation to both the water adlayers and the lithography patterns on graphene. EFM with dual pass technique, is used to study the electrostatic charge distribution of the ice-like water adlayers on the patterned graphene on Si substrate. During the first scan, the topography is collected and in the second scan, DC bias varying from +2V to -2V is applied between the sample (through CP-II AFM Proscan data acquisition software) and the conducting tip (SCM-PIT), in the unmounted chip carrier with counter electrode pin wire attachment. The tip is lifted by a height of 25 nm and DC cantilever deflection is monitored using EFM phase signal, due to the changes in the electrostatic force gradient.

3. Results and discussion

IC-AFM imaging was performed to identify few layer graphene (thickness 't' ~ 1.06 nm to 3.2 nm) and multi-layer graphene (thickness 't' ~ 4.69 nm to 6.5 nm) flakes placed on cleaned Si and SiO_2/Si substrates. Fig. 1a and b shows IC-AFM topography images of FLG (t = 1.63 nm) on Si and FLG (t = 1.11 nm) on

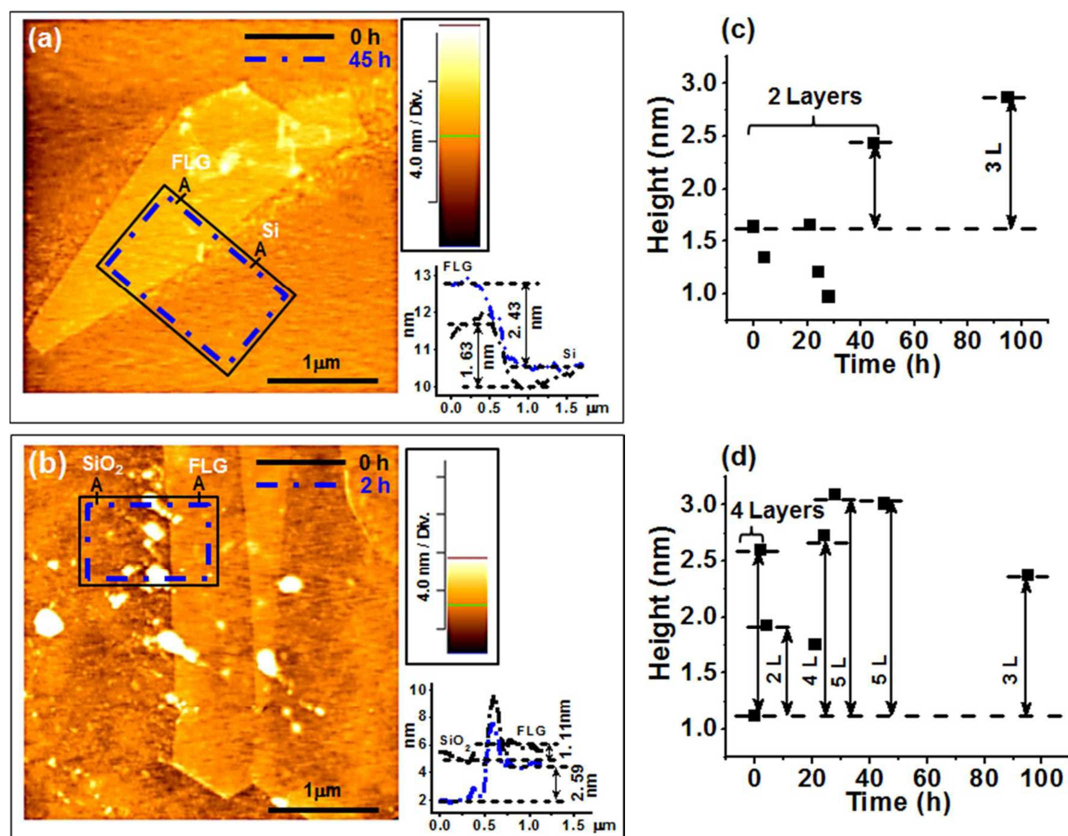

Fig. 1 Growth of ice-like water adlayers in between FLG on hydrophobic (Si) and FLG on hydrophilic (SiO_2) substrates when exposed to ambient humidity (51-52%) over several days: IC-AFM images for FLG (a) on Si and (b) on SiO_2 substrates; along with the average line profiles taken across points A-A marked in rectangles. Black solid line rectangle is at 0 h and blue dashed-dot rectangle is at the time of initial ice-adlayer formation. Plots of height of FLG flakes measured at different intervals of time (c) on Si and (d) on SiO_2 substrates.

Physical Chemistry Chemical Physics Accepted Manuscript

This journal is © The Royal Society of Chemistry 20xx

Please do not adjust margins

SiO_2/Si substrates. All the height measurements have been performed on un-processed topographic AFM images. AFM measurements of samples in air with heterogeneous water affinity have been reported to show artifacts in height measurements.[32, 33] However, in the present work, graphene flakes of uniform thickness in the measured regions would have uniform water affinity, at a fixed ambient RH. Hence, effects arising due to heterogeneous water affinity towards artifacts in height measurements may be minimal as both the surface of graphene and the substrate have more or less uniform water affinity. FLG on hydrophobic Si substrate shows clean surface devoid of water droplets as against FLG on hydrophilic SiO_2/Si substrate, which shows the presence of large droplets (height~19 nm, width~144 nm) of water on top of graphene and Si substrate. To check whether these sub-micron droplets features are related to water or tape residues, we performed contact mode imaging followed by IC-AFM imaging. The sub-micron droplets are swept across and do not remain fixed in the same position due to scanning in contact mode, implying that their origin is most likely related to water. In order to study the formation of ambient water adlayers in between FLG on hydrophobic Si and FLG on hydrophilic SiO_2/Si substrates, we performed IC-AFM imaging of the regions (see Fig. 1a and b) periodically and measured changes in the height of graphene with respect to the substrate over 95 h (see Fig. 1c and d). The marked solid line rectangle and dash-dot rectangles in Fig. 1a and b indicate the regions where the average line profiles measurements were made across A-A points at 0 h and at the time of initial IWL formation, respectively. The height changes of graphene are measured with respect to the initial (t = 0 h) graphene height. The 'dashed-lines' in the height versus time plots indicate the height of the IWL formed over time, with 'L' denoting the number of IWLs. For FLG on Si, the ice-like water bilayer is

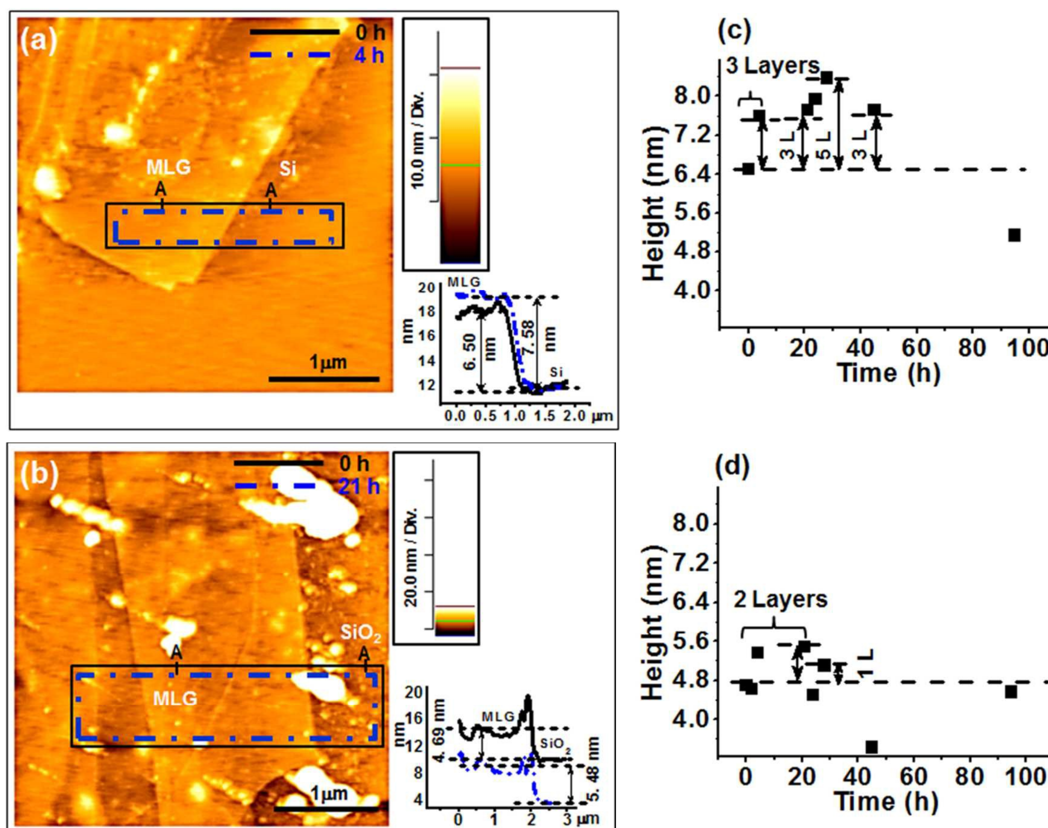

Fig. 2 Growth of ice-like water adlayers in between MLG on hydrophobic (Si) and MLG on hydrophilic (SiO_2) substrates when exposed to ambient humidity (51-52%) over several days: IC-AFM images for MLG (a) on Si and (b) on SiO_2 substrates; along with the average line profiles taken across points A-A marked in rectangles. Black solid line rectangle is at 0 h and blue dashed-dot rectangle is at the time of initial ice-adlayer formation. Plots of height of MLG flakes measured at different intervals of time (c) on Si and (d) on SiO_2 substrates.

 This journal is © The Royal Society of Chemistry 20xx

Please do not adjust margins

Physical Chemistry Chemical Physics Accepted Manuscript

formed after 45 h (see Fig. 1c) of exposure to ambient. This is determined by the changes in height of FLG of 1.63 nm at 0 h to 2.43 nm at 45 h (see averaged line profile in inset 1a) giving a height difference of 0.8 nm, which corresponds to the formation of a bi-layer of IWL.[16] Over 95 h, the height of the water adlayer is changed to 3 IWL. The regions of the p-doped Si surface not covered with graphene and exposed to ambient humidity, will result in dis-continuous native oxide growth on Si surface over time.[30] It is observed that the height of FLG on Si at 0 h is decreased over the first ~28 h by 0.3-0.66 nm, which may be on account of non-uniform native oxide growth on Si.[30] In contrast, FLG on SiO_2/Si shows change in height from 1.11 nm at 0 h to 2.59 nm after exposure to ambient, for 2 h (see average line profile in inset 1b), which corresponds to 4 IWL. Thereafter, there is slight variation in the number of IWL from 2-5, which may be on account of meta-stable nature of ice-water adlayers getting altered due to repetitive scanning in the same region.[31, 34]

Next, we studied MLG (t ~ 4.69-6.5 nm) on SiO_2/Si and Si substrates (see Fig. 2). For MLG (t ~ 6.5 nm) on Si substrate (see Fig. 2a), we found that 3 IWL (1.08 nm) are formed within 4 h of exposure to ambient (see Fig. 2c) as determined by the average line profile in Fig. 2a. On the other hand, a bi-layer of ice is formed between MLG and SiO_2/Si substrate only on exposure to ambient for a longer period of ~21 h, as shown in Fig. 2b and d. The height of MLG on SiO_2/Si shows a decrease from initial height of 4.69 nm, which may arise on account of increase in reference height of SiO_2/Si substrate due to the growth of water adlayers on SiO_2/Si surface itself.[35] After the initial IWL formation, the number of adlayers is altered over time due to repetitive scanning over the same region.

We observe ice-adlayer formation in between FLG as well as, MLG on both Si and SiO_2/Si substrates, as determined by the changes in height of graphene with respect to substrate on exposure to ambient humidity. FLG and MLG on Si and SiO_2/Si substrates show different time for the initial ice-adlayer formation as shown in Fig. 1 and 2. Since FLG is hydrophilic and MLG is hydrophobic in nature, we observe that when FLG (hydrophilic) is on top of Si (hydrophobic) substrate, it takes long time (45 h) for the initial ice-adlayer formation, due to the opposite affinity towards water for FLG and Si. In contrast, MLG (hydrophobic) on Si (hydrophobic) substrate takes shorter time (4 h) for the initial ice-adlayer formation due to similar affinity to water for both MLG and Si substrate. A similar trend, based on the affinity towards water, is observed

Table 1 Initial ice-adlayer formation for different FLG and MLG samples on Si and SiO_2/Si substrates

Samples	Initial Graphene Height (nm)	Δ H for Graphene @ initial ice-adlayer formation (nm)	Number of initial ice-adlayers	Time for initial ice-adlayer formation on	
				Si (Hydrophobic substrate)	SiO_2 / Si (Hydrophilic substrate)
1	1.066 (FLG)	0.359	1L	24 h	
2	1.634 (FLG)	0.798	2L	45 h	
3	3.050 (FLG)	2.59	7L	21 h	
4	1.116 (FLG)	1.482	4L		2 h
5	1.099 (FLG)	0.406	1L		2 h
6	3.207 (FLG)	0.357	1L		2 h
7	6.506 (MLG)	1.076	3L	4 h	
8	5.569 (MLG)	3.419	9L	4 h	
9	4.698 (MLG)	0.786	2L		21 h

Summarized Comparison of ice-adlayer formation for FLG and MLG on Si and SiO_2 substrates		
Number of Graphene layers	Initial ice-adlayer formation time	
	Hydrophobic substrate (Si)	Hydrophilic substrate (SiO_2)
FLG (1.11-1.63 nm)	45 h	2 h
MLG (4.69-6.50 nm)	4 h	21 h

Physical Chemistry Chemical Physics Accepted Manuscript

Please do not adjust margins

in the case of FLG and MLG on hydrophilic (SiO_2/Si) substrate, viz., 2 h for FLG on SiO_2/Si and 21h for MLG on SiO_2/Si substrate. This conclusion is based on a study performed on 9 different graphene flakes with different FLG and MLG thicknesses on Si and SiO_2/Si substrates, depicting a similar trend, as shown in Table 1.

The formation of ice-adlayer and its effect on AFM voltage nanolithographically-modified FLG and MLG surfaces on hydrophobic Si substrate (see Fig. 3) is also investigated. For this study, we chose graphene flake with neighboring FLG and MLG regions on Si substrate so as to simultaneously scan both FLG and MLG regions and minimize differing tip scanning effect for the meta-stable ice-adlayers. Trench lines on FLG (marked by dashed rectangle) and trench lines on MLG (marked by dashed circle) were made using contact-mode AFM voltage nanolithography. Average line profiles in Fig. 3a marked by solid line rectangle and dash-dot rectangle were taken simultaneously for both FLG and MLG on Si, as shown in the plots alongside the topography image for 0 h, 2 h and 10 h, to study the ice-adlayer formation on patterned FLG and MLG. There is a slight tilt observed in the average line profile at 0 h at the FLG terrace, which may be on account of edge to center growth of ice-like water adlayer, as reported earlier by Lee *et al.*[25]. With time, the tilt in the average line profile gets reduced at 2 h and 10 h, as more complete growth of IWLs takes place. From the average line profiles, it is seen that the height of FLG

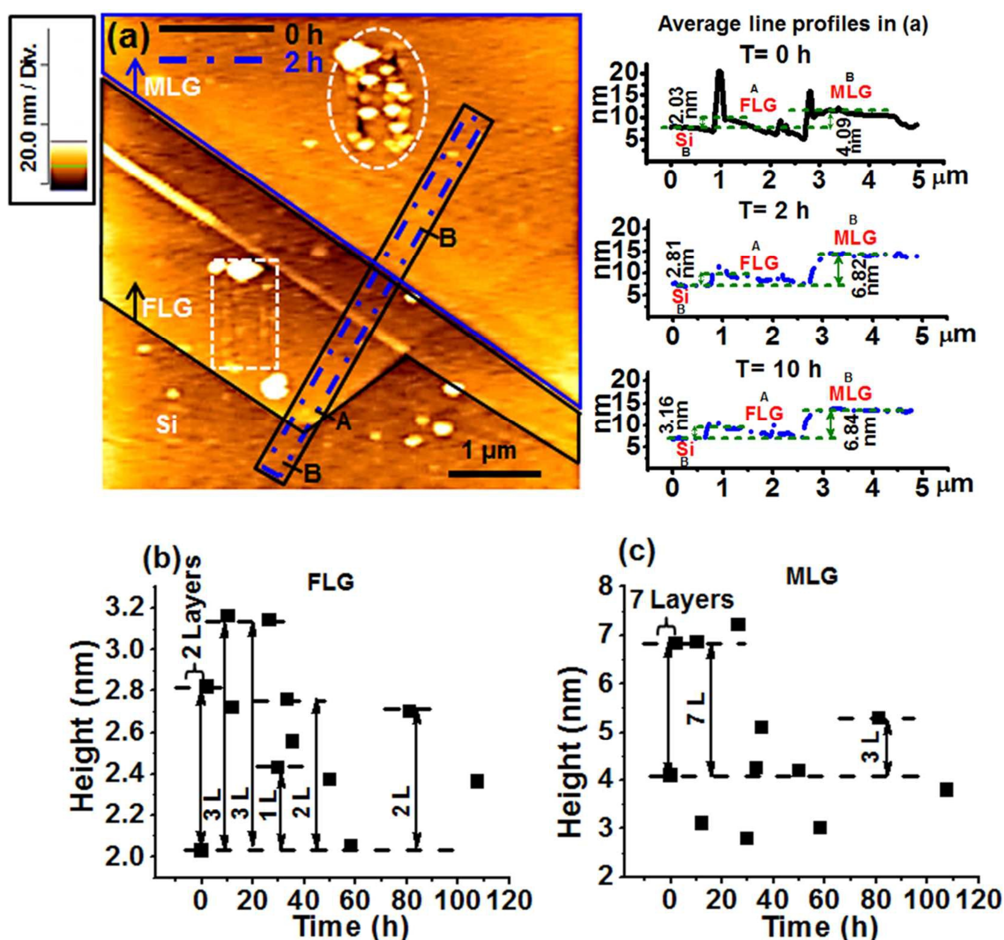

Fig. 3 Growth of ice-like water adlayers in between patterned FLG and MLG flakes on hydrophobic Si substrate exposed to ambient humidity (50-52%) over several days. Trench patterns are created using AFM voltage nanolithography with tip speed 0.01 μm/s, sample bias 10 V, set-point force 5 nN at ambient humidity of 50%: (a) IC-AFM image of patterned FLG trench region (enclosed by dash rectangle) and patterned MLG trench region (enclosed by dash circle) on Si substrate; the average line profiles shown alongside (a) are taken across points A-B for FLG and B-B for MLG, as shown in the marked rectangles. Black solid line rectangle is measurement at 0 h and blue dashed-dot rectangle is at the time of ice-adlayer formation at ~2 h and ~10 h. Plots of heights of (b) FLG and (c) MLG flakes measured on Si substrate at different time intervals. Two and seven ice-adlayers are formed within ~2 h for patterned FLG and MLG on Si, respectively.

 This journal is © The Royal Society of Chemistry 20xx

Physical Chemistry Chemical Physics Accepted Manuscript

Please do not adjust margins

(2.03 nm) at 0 h increases to 2.81 nm at 2 h, while as, for MLG the height changes from 4.09 nm at 0 h to 6.82 nm at 2 h. This indicates that the initial IWL is formed within the same time interval viz., 2 h, with 2 ice-adlayers being formed in the case of patterned FLG and 7 layers being formed for patterned MLG on Si, as shown in Fig. 3b and c. The ice-adlayers formation for patterned FLG and MLG is monitored over ~105 h. This shows that introducing defects on FLG and MLG on Si substrate induces quick formation of IWL irrespective of differing water affinity for FLG and MLG. The formed ice-adlayers are present over a long time (~80 h) though the numbers of ice-adlayers are altered due to their meta-stable nature.

To investigate the effect of ice-adlayers formation on the lithography trench patterns on FLG and MLG, a study of the changes in the trench width dimensions and the charged nature of the lithography trench patterns on FLG and MLG regions were made over ~4 days (105 h). From the IC-AFM topography images, it is evident that the trench patterns 1 and 2 on FLG and trench patterns 3 and 4 on MLG show a visual increase in the width of the dimensions (see Fig. 4a-d). The normalized changes in trench width ($\Delta W/W_0 \times 100$) were monitored to study the nature of the changes. In the case of FLG, over the first 27 h, there is a sharp increase in width of the trench patterns 1 and 2, and thereafter, minimal changes are observed (see Fig. 4e). In contrast, the trench patterns 3 and 4 on MLG show a steady small linear rate of change in the normalized trench width over the entire ~4 days (105 h) as shown in Fig. 4f. The effect of the presence of initial adlayers over ~ a day (27 h), in the case of FLG (2-3 ice-adlayers) leads to a sharp increase of ~ 37-41%, while as, in the case of MLG (7 ice-adlayers) leads to a linear increase of ~ 41-54% for the two trenches created.

In order to understand the role of the initial ambient IWL on the trench width dimension changes, we performed EFM study of the patterned FLG and MLG regions on hydrophobic Si substrate. Un-patterned regions of FLG and MLG show coulombic behavior as seen by the opposite dark and bright EFM contrast (see Fig. 5a and b) for $\pm$ 2V. This is verified in terms of opposite sign in the phase shift values, shown in ESI, Fig. S1a and b. The evolution of the charged nature of un-patterned regions of FLG and MLG is studied by measuring the normalized changes in EFM phase shift ($\Delta\Phi/\Phi_0$) values with time (see Fig. 5c and d). $\Delta\Phi/\Phi_0$ versus ΔT plots show the response for positive and negative voltages for un-patterned

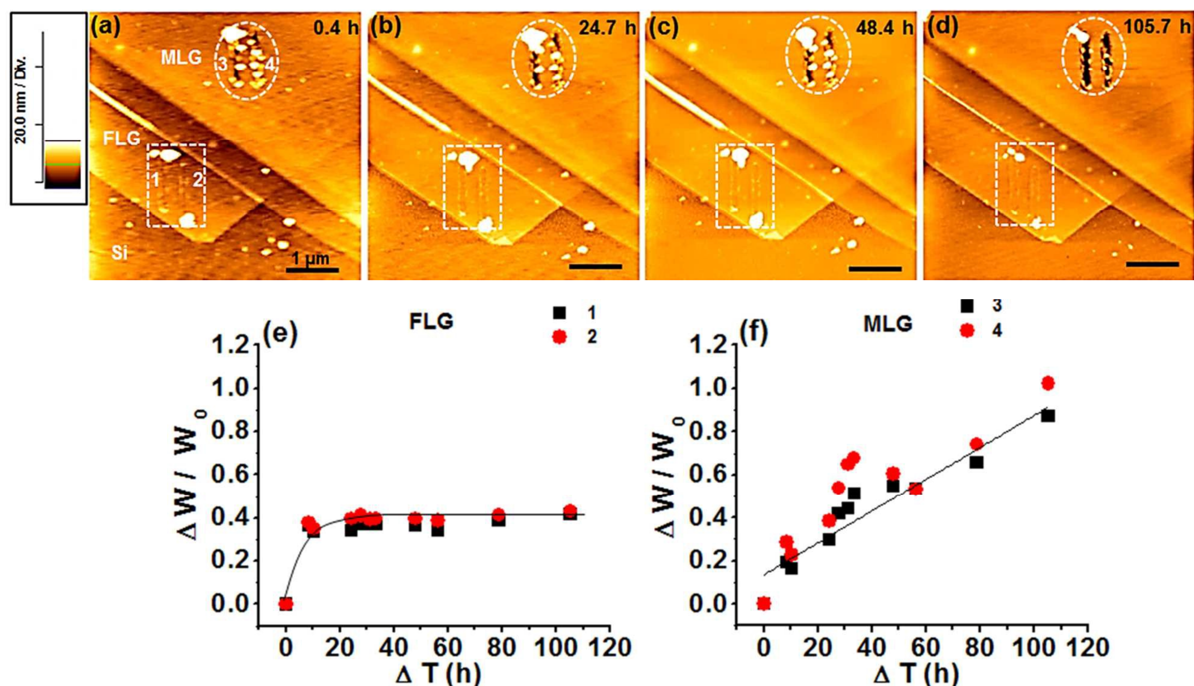

Fig. 4 IC-AFM topography images showing evolution of width of trench patterns 1 and 2 on FLG and 3 and 4 on MLG on Si substrate, enclosed in dashed rectangle and circle, respectively, obtained at (a) 0.4 h, (b) 24.7 h, (c) 48.4 h, and (d) 105.7 h since lithography time. Scale bar=1μm. The normalized changes in trench width ($\Delta W / W_0 \times 100$) for (e) FLG, shows a sharp increase of ~ 37-41% (over ~27 h) due to the presence of initial 2-3 ice-adlayers; and (f) MLG, shows a steady linear rate of increase due to the presence of initial 7 ice-adlayers.

Physical Chemistry Chemical Physics Accepted Manuscript

Please do not adjust margins

Physical Chemistry Chemical Physics Accepted Manuscript

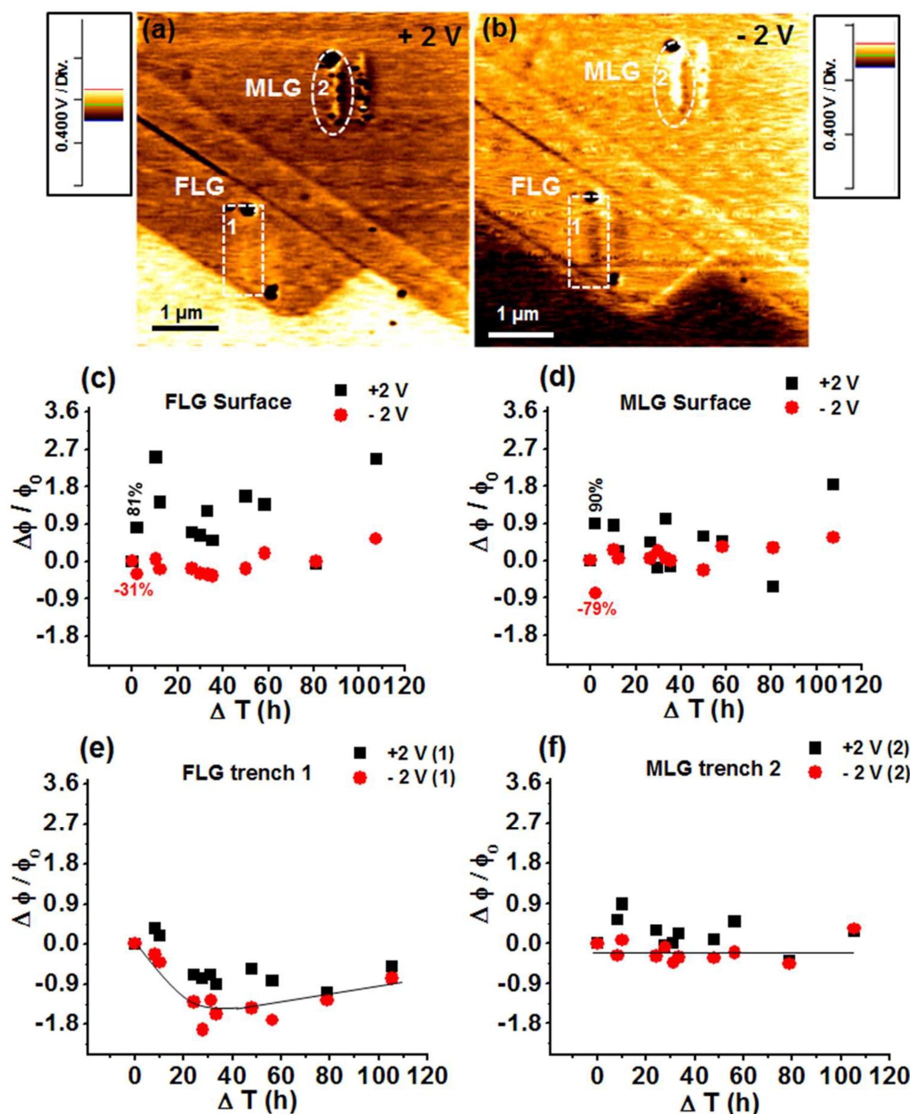

Fig. 5 EFM images of patterned FLG, MLG on Si substrate for (a) +2 V and (b) -2 V. Un-patterned FLG and MLG regions show dark (+2 V) and bright (-2 V) contrast with bias reversal, while as trench 1 on FLG region shows bright (+2 V) and dark (-2 V) EFM contrast, pointing to coulombic behavior. Trench 2 on MLG region shows bright contrast upon bias polarity reversal implying capacitive behavior. Plots of normalized changes in EFM phase shift ($\Delta\Phi/\Phi_0$ x 100) with time for (c) FLG surface, showing changes of -31% (-2V) and 81% (+2V) over ~2 h; (d) MLG surface, showing changes of -79% (-2 V) and 90% (+2 V) over ~2 h, on account of initial ice-adlayers formation and thereafter show random EFM phase shift variations with time; (e) trench 1 created on FLG, showing a sharp decrease in charge dissipation of 78% (+2V) and 194% (-2V) over ~27 h, due to initial ~2 ice-adlayers and (f) trench 2 created on MLG, showing a constant small rate of change in charge dissipation over ~105 h, due to initial ~7 ice-adlayers formation.

regions of FLG and MLG. Graphene is negatively charged as it shows dark contrast (attractive interaction) on application of positive voltage during EFM. As the number of layers in graphene increases viz., FLG to MLG, the EFM phase shift values also show an increase[12, 23] (see ESI, Fig. S1a and b). Due to the difference in the initial ice-adlayers formation over 2 h, in the case of FLG surface (~2 ice-adlayers) and MLG surface (~7 ice-adlayers), the corresponding changes in normalized EFM phase shift ($\Delta\Phi/\Phi_0\times100$) for FLG is -31% (-2V) and 81% (+2V), and for MLG it is -79% (-2V) and 90% (+2V). The changes for MLG surface in $\Delta\Phi/\Phi_0\times100$ for negative bias (-2V), are more on account of the higher viz., 7 ice-adlayers formed.

 This journal is © The Royal Society of Chemistry 20xx

Please do not adjust margins

Thereafter, the changes are random for both un-patterned regions of FLG and MLG, due to the variation in the number of ice-adlayers, on account of repeated scanning of same region.

The trench pattern 1 on FLG (enclosed in dashed rectangle) shows opposite contrast viz., bright (+2V) and dark (-2V) while as, trench pattern 2 on MLG (enclosed dashed circle) shows similar bright contrast on bias polarity reversal (see Fig. 5a and b). We observe opposite sign EFM phase shift values for FLG trench pattern and same positive sign EFM phase shift (Φ) values for MLG trench on bias polarity reversal upto ~ 27 h (See ESI, Fig. S2 and 3). Hence, the FLG trench pattern shows a coulombic nature with a sharp decrease in normalized EFM phase shift (charge) over 27 h, while as, the MLG trench pattern shows capacitive behavior with a constant small rate of change in decrease of charge over the entire ~105 h. These trends in charge dissipation observed for FLG and MLG trenches in the EFM analysis are in accordance with the topography changes observed for the width of FLG and MLG trenches patterns.

4. Conclusions

We report the growth of ice-like water adlayers in between mechanically exfoliated FLG, MLG flakes on hydrophobic Si and hydrophilic SiO_2/Si substrates when exposed to ambient over several days. Our observations show that the time taken for the initial ice-adlayers formation for the as-prepared FLG on hydrophobic Si substrate is ~45 h, while as, for hydrophilic SiO_2/Si substrate, it is ~2 h. In contrast, for the as-prepared MLG, the initial ice-adlayers is formed on hydrophobic Si substrate within ~4 h, while as, on hydrophilic SiO_2/Si substrate, it takes longer time ~21 h. This is the first report of the growth time of initial ice-adlayer formation being dependent on the nature of graphene viz., FLG (hydrophilic) and MLG (hydrophobic) with respect to the water affinity for the underlying substrates. For similar affinity towards water, it takes shorter time for the initial ice-adlayer formation, as against for dis-similar affinity. However, this trend in the difference in initial ice-adlayer formation time breaks down, in the case of patterned (defected) FLG and MLG flakes on Si. It is observed that trench patterns created using AFM voltage nanolithography on FLG and MLG on Si substrate induce quick formation of initial ice–like water adlayers, with FLG showing fewer initial ice-adlayers (2 layers), while as, for MLG, 7 initial ice-adlayers are formed over a short period of ~2 h.

The presence of these initial ice-adlayers on patterned FLG and MLG over a time period of several days, leads to modification of the initial lithography pattern dimensions, as observed for HOPG in our earlier work. The rate of change in dimensions varies depending on the number of initial ice-adlayers formed. For FLG on Si, there is a sharp increase (37-41%) in the width of the trench pattern over ~a day and thereafter, not much variation was observed for over ~4days. In the case of MLG on Si, there is a linear rate of increase over the entire period of ~4days. The sharp increase in the width of the FLG trench patterns may be on account of two initial ice-adlayers being more polarized, as compared to seven initial ice-adlayers on MLG on Si. This is confirmed by the EFM analysis of the bare regions of FLG and MLG and the trench patterns on FLG and MLG surfaces, where bare MLG regions show higher rate of change of EFM phase shift values than the corresponding FLG surface, over the first two hours, due to higher number of initial ice-adlayers. For the patterned FLG, the sharp decrease in rate of change of EFM phase shift implies corresponding sharp charge dissipation, causing fast etching reaction, giving rise to a sharp increase in the trench width dimension over a day. The patterned MLG, on the other hand shows a small and constant rate of change of EFM phase shift values implying a linear change in the trench width dimension. Hence, the growth time and the number of ice-adlayers formed are dependent on the nature of graphene and the underlying substrates and have a significant contribution on the dynamics of the dimension and the charged nature of lithographically patterned graphene. Such changes caused due to the presence of initial ice-adlayers for graphene based devices on technologically important Si and SiO_2/Si substrates will have important implications for their performance.

Acknowledgements

This work was supported in part by VIT University, Vellore and Department of Science and Technology, Nanomission, New Delhi. T. G. and G. T. acknowledge the financial support from VIT University. T. G., G. T., G. J. and G. R. are thankful to Prof. J. P. Raina, Emeritus Professor, Center for Nanotechnology Research, VIT University, for his constant encouragement.

Notes and references

1 K. S. Novoselov, A. K. Geim, S. V. Morozov, D. Jiang, Y. Zhnag, S. V. Dubonos, I. V. Grigorieva and A. A. Firsov, *Science*, 2004, **306**, 666-669.
2 T. Roy, M. Tosun, J. S. Kang, A. B. Sachid, S. B. Desai, M. Hettick, C. C. Hu and A. Javey, *ACS Nano*, 2014, **8**, 6259-6264.
3 U. Jung, Y. G. Lee, C. G. Kang, S. Lee, J. J. Kim, H. J. Hwang, S. K. Lim, M. H. Ham and B. H. Lee, *Sci. Rep.*, 2014, **4**, 4886.
4 C. C. Chen, M. Aykol, C. C. Chang, A. F. J. Levi and S. B. Cronin, *Nano Lett.*, 2011, **11**, 1863-1867.
5 N. Kurra, R. G. Reifenberger and G. U. Kulkarni, *ACS Appl. Mater. Interfaces*, 2014, **6**, 6147-6163.
6 C. Yu, H. Liu, W. Ni, N. Gao, J. Zhao and H. Zhang, *Phys. Chem. Chem. Phys.,* 2011, **13**, 3461-3467.
7 P. Li, C. Chen, j. Zhang, S. Li, B. Sun and Q. Bao, *Front. Mater.*, 2014, **1**, 1-7.
8 F. Yavari and N. Koratkar, *J. Phys. Chem. Lett.*, 2012, **3**, 1746-1753.
9 G. Yang, C. Lee, J. Kim, F. Ren and S. J. Pearton, *Phys. Chem. Chem. Phys.*, 2013, **15**, 1798-1801.
10 P. Y. Chen, H. Huang, D. Akinwande and A. Alù, *ACS Photonics*, 2014, **1**, 647-654.
11 O. Ochedowski, B. K. Bussmann and M. Schleberger, *Sci. Rep.*, 2014, **4**, 6003.

Physical Chemistry Chemical Physics Accepted Manuscript

Please do not adjust margins

12 O. Kazakova, V. Panchal and T. L. Burnett, *Crystals*, 2013, **3**, 191-233.
13 H. Komurasaki, T. Tsukamoto, K. Yamazaki and T. Ogino, *J. Phys. Chem. C*, 2012, **116**, 10084-10089.
14 J. Shim, C. H. Lui, T. Y. Ko, Y. J. Yu, P. Kim, T. F. Heinz and S. Ryu, *Nano Lett.*, 2012, **12**, 640-654.
15 Y. Yang, K. Brenner and R. Murali, *Carbon*, 2012, **50**, 1727-1733.
16 K. Xu, P. Cao and J. R. Heath, *Science*, 2010, **329**, 1188-1191.
17 K. T. He, J. D. Wood, G. P. Doidge, E. Pop and J. W. Lyding, *Nano Lett.*, 2012, **12**, 2665-2672.
18 B. Rezania, M. Dorn, N. Severin and J. P. Rabe, *J. Colloid Interface Sci.*, 2013, **407**, 500-504.
19 J. S. Kim, J. S. Choi, M. J. Lee, B. H. Park, D. Bukhvalov, Y.W. Son, D. Yoon, H. Cheong, J. N. Yun, Y. Jung, J. Y. Park and M. Salmeron, *Sci. Rep.*, 2013, **3**, 1-6.
20 M. Cheng, D. Wang, Z. Sun, J. Zhao, R. Yang, G. Wang, W. Yang, G. Xie, J. Zhang, P. Chen, C. He, D. Liu, L. Xu, D. Shi, E. Wang and G. Zhang, *ACS Nano*, 2014, **8**, 3955-3960.
21 J. Moser, A. Verdaguer, D. Jiménez, A. Barrerio and A. Bachtold, *Appl. Phys. Lett.*, 2008, **92**, 123507-1-3.
22 F. Yavari, C. Kritzinger, C. Gaire, L. Song, H. Gullapalli, T. Borca-Tasciuc, P. M. Ajayan and N. Koratkar, *Small*, 2010, **6**, 2535-2538.
23 G. L. Hao, X. Qi, J. Li., L. W. Yang, J. J. Yin, F. Lu and J. X. Zhong, *Solid State Commun.*, 2011, **151**, 818-821.
24 M. J. Lee, J. S. Choi, J. S. Kim, I.S. Byun, D. H. Lee, S. Ryu, C. Lee and B. H. Park, *Nano Res.*, 2012, **5**, 710-717.
25 D. Lee, G. Ahn and S. Ryu, *J. Am. Chem. Soc.*, 2014, **136**, 6634-6642.
26 A. Verdaguer, J. J. Segura, L. López-Mir, G. Sauthier and J. Fraxedas, *J. Chem. Phys.*, 2013, **138**, 121101-1-4.
27 M. Temmen, O. Ochedowski, M. Schleberger, M. Reichling and T.R.J. Bollmann, *New J. Phys.*, 2014,**16**, 053039.
28 Z. Xu, Z. Ao, D. Chu, A. Younis, C. Ming and S. Li, *Sci. Rep.*, 2014, **4**, 6450.
29 X. Feng, S. Maier and M. Salmeron, *J. Am. Chem. Soc.*, 2012, **134**, 5662-5668.
30 O. Ochedowski, G. Begall, N. Scheuschaner, M. E. Kharrazi, J. Maultzsch and M. Schleberger, *Nanotechnology*, 2012, **23**, 405708.
31 T. Gowthami, N. Kurra and G. Raina, *Nanotechnology*, 2014, **15**, 155304.
32 S. Santos, A. Verdaguer and M. Chiesa, *J. Chem. Phys.*, 2012, **137**, 044201-1-14.
33 A. Verdaguer, S. Santos, G. Sauthier, J. J. Segura, M. Chiesa and J. Fraxedas, *Phys. Chem. Chem. Phys.*, 2012, **14**, 16080-16087.
34 A. Verdaguer, G. M. Sacha, H. Bluhm and M. Salmeron, *Chem. Rev.*, 2006, **106**, 1478-1510.
35 A. Verdaguer, C. Weis, G. Oncins, G. Ketteler, H. Bluhm and M. Salmeron, *Langmuir*, 2007, **23**, 9699-9703.

Physical Chemistry Chemical Physics Accepted Manuscript

This journal is © The Royal Society of Chemistry 20xx

Please do not adjust margins